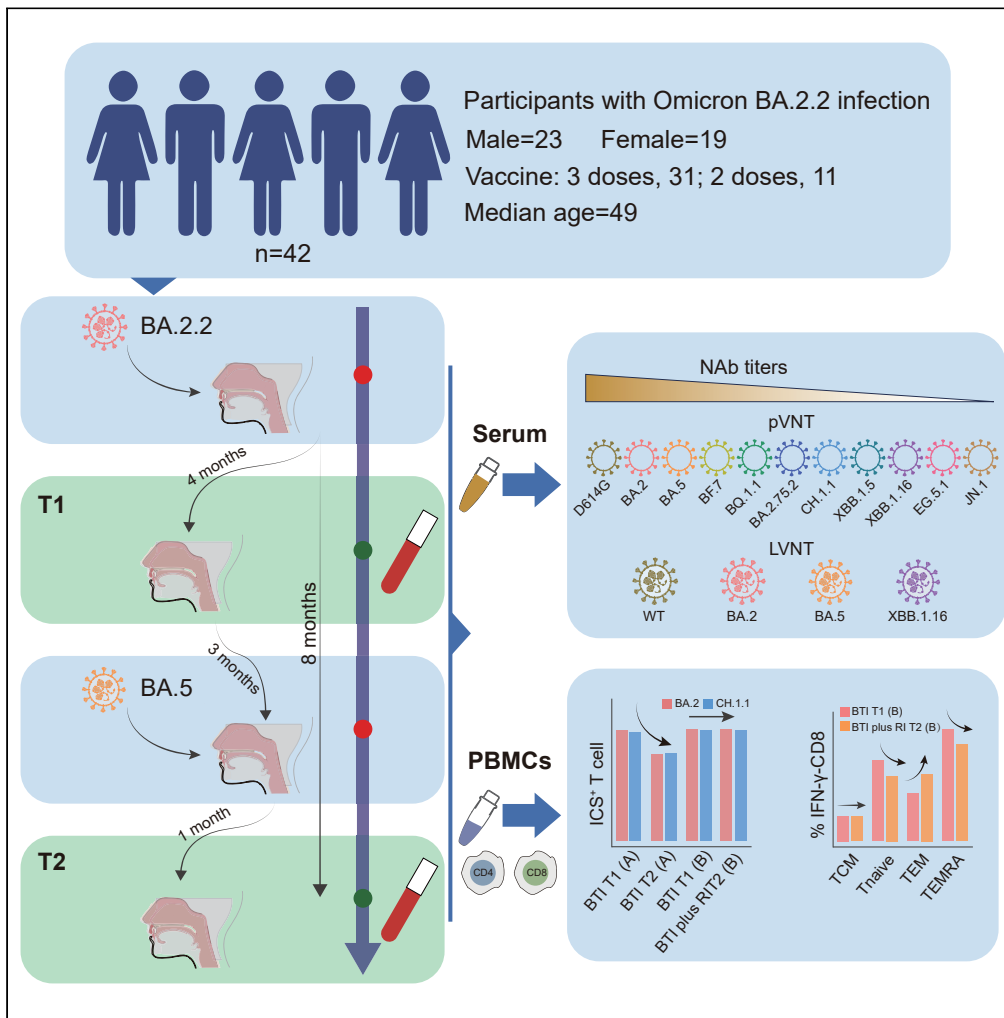


Article

# Humoral and cellular immune responses following Omicron BA.2.2 breakthrough infection and Omicron BA.5 reinfection



Xin-Jing Zhao, Bin Ji, Chao Shang, ..., Xiao Li, Guo-Lin Wang, Li-Qun Fang

geno0109@vip.sina.com (H.W.)  
 skyllee6226@163.com (X.L.)  
 guolin\_wang2019@163.com (G.-L.W.)  
 fang\_lq@163.com (L.-Q.F.)

**Highlights**

Levels of IgG and NAbs decrease continuously post BTI and correlate with reinfection

T cells well-recognize both Omicron BA.2 and CH.1.1 peptides post BTI and reinfection

Omicron subvariant reinfection enhance virus-specific ICS<sup>+</sup> T cell responses

Omicron subvariant reinfection promote the differentiation of memory CD8<sup>+</sup> T cells



## Article

## Humoral and cellular immune responses following Omicron BA.2.2 breakthrough infection and Omicron BA.5 reinfection

Xin-Jing Zhao,<sup>1,2,6</sup> Bin Ji,<sup>3,6</sup> Chao Shang,<sup>4,6</sup> De-Yu Li,<sup>2,6</sup> Sheng Zhang,<sup>2</sup> Hong-Jing Gu,<sup>2</sup> Hong-Hong Peng,<sup>3</sup> Cheng Qian,<sup>5</sup> Cui-Ling Zhang,<sup>4</sup> Chao Shi,<sup>3</sup> Yuan Shen,<sup>3</sup> Jin-Jin Chen,<sup>2</sup> Qiang Xu,<sup>2</sup> Chen-Long Lv,<sup>2</sup> Bao-Gui Jiang,<sup>2</sup> Hui Wang,<sup>2,\*</sup> Xiao Li,<sup>4,\*</sup> Guo-Lin Wang,<sup>2,7,\*</sup> and Li-Qun Fang<sup>1,2,\*</sup>

## SUMMARY

The emergence of novel Omicron subvariants has raised concerns regarding the efficacy of immunity induced by prior Omicron subvariants breakthrough infection (BTI) or reinfection against current circulating Omicron subvariants. Here, we prospectively investigated the durability of antibody and T cell responses in individuals post Omicron BA.2.2 BTI, with or without subsequent Omicron BA.5 reinfection. Our findings reveal that the emerging Omicron subvariants, including CH.1.1, XBB, and JN.1, exhibit extensive immune evasion induced by previous infections. Notably, the level of IgG and neutralizing antibodies were found to correlate with subsequent Omicron BA.5 reinfection. Fortunately, T cell responses recognizing both Omicron BA.2 and CH.1.1 peptides were observed. Furthermore, Omicron BA.5 reinfection may alleviate immune imprinting induced by WT-vaccination, bolster virus-specific ICS<sup>+</sup> T cell responses, and promote the phenotypic differentiation of virus-specific memory CD8<sup>+</sup> T cells. Anti-gen-updated or T cell-conserved vaccines are needed to control the transmission of diverse emerging SARS-CoV-2 variants.

## INTRODUCTION

Severe acute respiratory syndrome coronavirus 2 (SARS-CoV-2) causes a continuous burden of morbidity and mortality. While immunity elicited by wild-type (WT) vaccination or prior Omicron infection remains pivotal in mitigating severe disease, it exhibits diminished or absent neutralizing antibody (NAb) activity against the emerging Omicron subvariants, particularly BQ.1.1, BA.2.75.2, CH.1.1, XBB, and BA.2.86 subvariants.<sup>1–6</sup> Therefore, whether the patients with the previous Omicron subvariant infection still maintain humoral and cellular immunity to prevent themselves from reinfection or severe disease from newly emerging Omicron subvariants is of paramount concern.

Previous studies have reported that breakthrough infection (BTI) caused by Omicron BA.1, BA.2, or BA.5 can induce broadly neutralizing antibodies against previous variant of concerns (VOCs) and BA.2-derived Omicron subvariants. However, they show diminished NAb titers against BQ.1.1, BA.2.75.2, CH.1.1, XBB, and BA.2.86 subvariants during the early convalescent stage.<sup>7–21</sup> Yet, only limited studies focused on the durability of immunity beyond 6 months post Omicron subvariants BTI,<sup>22,23</sup> with a notable decline of antibody response against emerging Omicron subvariants. Moreover, serum antibodies have been demonstrated to confer protection against infection by reducing viral load and hastening viral clearance.<sup>24–26</sup> Therefore, given the declining NAb titers, individuals with previous Omicron subvariants infection are at a high risk of reinfection.

Considering the significant decline in antibody responses post infection or vaccination, a thorough investigation into the persistence of memory T cell immune responses is imperative. Previous studies have shown the pivotal role of SARS-CoV-2 specific T cell responses in virus control at very early stage, correlating inversely with upper airway viral load during acute infection pre-seroconversion.<sup>27–29</sup> Moreover, evidences have suggested that the majority of T cell responses induced by vaccination or infection exhibit cross-recognize reactivity against various SARS-CoV-2 variants, including both WT and Omicron strains.<sup>18,20,30,31</sup> Regarding the potential future reinfection with diverse

<sup>1</sup>Department of Epidemiology and Biostatistics, School of Public Health, Anhui Medical University, Hefei, China

<sup>2</sup>State Key Laboratory of Pathogen and Biosecurity, Academy of Military Medical Science, Beijing, P.R. China

<sup>3</sup>Department of Disease Control, the Affiliated Wuxi Center for Disease Control and Prevention of Nanjing Medical University, Wuxi Center for Disease Control and Prevention, Wuxi, China

<sup>4</sup>Changchun Veterinary Research Institute, Chinese Academy of Agricultural Sciences, Changchun, China

<sup>5</sup>Jiangyin Center for Disease Control and Prevention, Jiangyin, China

<sup>6</sup>These authors contributed equally.

<sup>7</sup>Lead contact

\*Correspondence: [geno0109@vip.sina.com](mailto:geno0109@vip.sina.com) (H.W.), [skylee6226@163.com](mailto:skylee6226@163.com) (X.L.), [guolin\\_wang2019@163.com](mailto:guolin_wang2019@163.com) (G.-L.W.), [fang\\_lq@163.com](mailto:fang_lq@163.com) (L.-Q.F.)  
<https://doi.org/10.1016/j.isci.2024.110283>



Omicron subvariants, it is urgent to study whether the T cell response elicited by early Omicron BA.2 BTI can effectively cross-recognize emerging Omicron subvariants, and whether the reinfection with Omicron subvariant can enhance T cell responses.

Overall, comprehensive investigations into the immunological characteristics of COVID-19 patients affected by Omicron subvariants BTI and subsequent reinfections remain scarce.<sup>32,33</sup> Hence, we conducted a longitudinal study involving 42 COVID-19 patients at both 4- and 8-month post Omicron BA.2.2 BTI. In our previous study, partial results regarding antibody responses against several SARS-CoV-2 variants were reported.<sup>34</sup> Herein, we systematically tested serum IgG and NAb antibody responses against various emerging Omicron subvariants and clarified the cross-reactivity of activation of T cell responses against different Omicron peptide pools. These findings furnish critical insights into the persistence of immunity following Omicron BTI and the potential cross-reactivity of previous Omicron infection against emerging Omicron subvariants.

## RESULTS

### Study participants and clinical characteristics

A cohort of 42 vaccinated participants with confirmed Omicron BA.2.2 infections was enrolled to investigate humoral immunity persistence and T cells cross-reactivity in Jiangyin city, Jiangsu Province of China between September 19 and November 08, 2022 (Table 1; Figure 1). The median age of our participants was 49.0 (IQR, 41.0–53.0); 23 (54.8%) subjects were male and 19 (45.2%) subjects were female. Thirty-one (73.8%) subjects received three doses of CoronaVac/BBIBP-CorV vaccines while 11 (26.2%) subjects received two doses of CoronaVac/BBIBP-CorV vaccines. All individuals diagnosed with COVID-19 infection either had confirmed BA.2.2 infection through sequencing or were linked to Omicron BA.2.2 sequence-confirmed cases based on the epidemiological investigation. Between January 06 and February 01, 2023, a total of 26 subjects were followed-up for data and sample collection. Two followed-up visits were conducted for these participants at median intervals of 138.5 days (IQR, 137.0–139.3) and 249.0 days (IQR, 247.8–255.0) after the onset of Omicron BA.2.2 BTI. Serum samples and peripheral blood mononuclear cells (PBMCs) were collected from the participants during each visit. At 8-month post Omicron BA.2.2 BTI, fourteen participants experienced reinfection with Omicron BA.5 were visited between December 2022 and January 2023, whose infection was confirmed by self-antigen test twice a week and timely surveillance data of circulating SARS-CoV-2 variants (Figure S1). The detailed information about sex, age, vaccination background, and infection status of each participant can be found in Table S1. Additionally, ten vaccinated subjects without infection were enrolled as healthy controls (Table 1).

Based on the visited time points and infection status, we categorized the participants into the following groups: vaccinated healthy control (VachC) group (1.5 months after vaccination with 2/3-dose inactivated vaccines), BTI T1 group (4-month after Omicron BA.2.2 BTI,  $n = 42$ ), BTI T1 (A) group (4-month after Omicron BA.2.2 BTI without subsequently Omicron BA.5 reinfection,  $n = 12$ ), BTI T1 (B) group (4-month after Omicron BA.2.2 BTI with subsequently Omicron BA.5 reinfection,  $n = 14$ ), BTI T2 (A) group (8-month after Omicron BA.2.2 BTI without Omicron BA.5 reinfection,  $n = 12$ ), BTI plus RI T2 (B) group (8-month after Omicron BA.2.2 BTI with Omicron BA.5 reinfection,  $n = 14$ ) (Figure 1).

### Omicron subvariants BTI and reinfection can induce robust Omicron BA.2- and BA.5-specific binding IgG antibodies

We firstly investigated the levels of binding IgG antibodies among the participants. The data revealed that 95.2% and 85.7% of individuals in BTI T1 group had detectable spike-specific binding IgG antibodies against Omicron BA.2 and BA.5, respectively (Figure 2A). At 8 months after Omicron BA.2.2 BTI, 100% and 58.3% subjects in BTI T2 (A) group had detectable Omicron BA.2- and BA.5-specific binding IgG antibodies, while all subjects in BTI plus RI T2 (B) group had detectable binding IgG antibodies against both Omicron BA.2 and BA.5 (Figure 2A). Furthermore, the level of spike-specific IgG antibodies against Omicron BA.5 was significantly lower than that against Omicron BA.2 in different groups, indicating reduced cross-reactivity between different Omicron subvariants (Figure 2A). When comparing the binding IgG antibodies between groups of VachC, BTI T1 (A), BTI T2 (A), BTI T1 (B), and BTI plus RI T2 (B), we found that subjects with Omicron BA.2.2 BTI and/or BA.5 reinfection had higher levels of binding IgG antibodies than those in VachC group, even 8 months after Omicron BA.2.2 infection in BTI T2 (A) group (Figure 2B). Further comparison at different visited time points showed that subjects in BTI T2 (A) group had significantly lower IgG antibodies than that in BTI T1 (A) group, while BTI plus RI T2 (B) group had significantly higher IgG antibodies than that in BTI T1 (B) group, suggesting that Omicron BA.5 reinfection can elevate binding IgG antibody titers (Figure 2B). In addition, subjects in BTI T1 (B) group had significantly lower binding IgG antibody titers against both Omicron BA.2 and BA.5 than that in BTI T1 (A) group, revealing that the level of binding IgG antibodies was correlated with the subsequent Omicron BA.5 reinfection (Figure 2B).

### Omicron BA.5 reinfection can enhance the neutralizing ability against emerging Omicron subvariants

We then assessed the neutralizing ability of serum among participants by pseudovirus neutralization test (pVNT) using various SARS-CoV-2 variants spike plasmids with specific mutations (Figure S2). We firstly compared the NAb titers against the D614G and various Omicron subvariants at the same followed-up time points (Figure 3A). Overall, compared with the D614G, the serum NAb titers were comparable against Omicron BA.2, and slightly decreased against Omicron BA.5 and BF.7, while the NAb titers against Omicron BQ.1.1, BA.2.75.2, CH.1.1, XBB.1.5, XBB.1.16, EG.5.1, and JN.1 subvariants were significantly reduced. In detail, the NAb titers against Omicron BA.2, BA.5, and BF.7 that were 2.0–5.8 times lower than those against D614G, while the NAb titers against other seven Omicron subvariants that were 25.8–84.5 times lower than those against D614G in BTI T1 group. Over 90% participants in BTI T1 group had detectable antibodies against D614G, BA.2, BA.5, and BF.7, 40–70% participants had detectable antibodies against BQ.1.1, BA.2.75.2, and XBB.1.16, while only 7–20% serum from participants could neutralize CH.1.1, XBB.1.5, EG.5.1, and JN.1. In BTI T2 (A) group, the NAb titers against Omicron BA.2,

**Table 1. Characteristics of study participants**

	COVID-19 (n = 42)	Healthy controls (n = 10)
Age (median, IQR)	49.0 (41.0–53.0)	40.5 (31.8–56.5)
Sex (n, %)		
Male	23 (54.8)	5 (50.0)
Female	19 (45.2)	5 (50.0)
Vaccination (n, %)		
First dose		
CoronaVac	22 (52.4)	6 (60.0)
BBIBP-CorV	20 (47.6)	4 (40.0)
Second dose		
CoronaVac	23 (54.8)	10 (100)
BBIBP-CorV	19 (45.2)	0 (0)
Third dose		
CoronaVac	11 (26.2)	3 (30.0)
BBIBP-CorV	20 (47.6)	4 (40.0)
unvaccinated	11 (26.2)	3 (30.0)
Clinical symptoms after Omicron BA.2.2 BTI (n, %)		
Asymptomatic	20 (47.6)	N/A
Symptomatic	22 (52.4)	N/A
Fever	16 (72.7)	N/A
Cough	9 (40.9)	N/A
Sore throat	6 (27.3)	N/A
Headache	3 (13.6)	N/A
Fatigue	2 (9.1)	N/A
Runny nose	1 (4.5)	N/A
Muscle pain	1 (4.5)	N/A
Diarrhea	1 (4.5)	N/A
Clinical symptoms after Omicron BA.5 RI (n, %)		
Asymptomatic	10 (71.4)	N/A
Symptomatic	4 (28.6)	N/A
Runny nose	2 (50.0)	N/A
Muscle pain	2 (50.0)	N/A
Fever	1 (25.0)	N/A
Cough	1 (25.0)	N/A
Days between last vaccination and BTI (median, IQR)	139.5 (103.8–146.3)	N/A
Sampling time (median, IQR)		
Days between BTI/vaccination and 1 <sup>st</sup> visit <sup>a</sup>	138.5 (137.0–139.3)	42.5 (17.3–60.0)
Days between BTI and 2 <sup>ND</sup> visit	249.0 (247.8–255.0)	N/A
Days between 1 <sup>st</sup> visit and RI	85.5 (83.0–90.0)	N/A
Days between BTI and RI	224.0 (221.5–229.0)	N/A
Days between RI and 2 <sup>ND</sup> visit	27.0 (24.5–43.0)	N/A

BTI, breakthrough infection. RI, reinfection. N/A, not applicable.

<sup>a</sup>Days between last vaccination and sampling for healthy controls.

BA.5, and BF.7 that were 1.6–3.7 times lower than those against D614G, while the NAb titers against other seven Omicron subvariants that were 21.3–85.0 times lower than those against D614G. All of the participants in BTI T2 (A) group had detectable NAb against D614G, BA.2, BA.5, and BF.7, while lower prevalence of 75.0%, 41.7%, 16.7%, 8.3%, 0%, 0%, and 0% serum from participants neutralized BQ.1.1, BA.2.75.2,

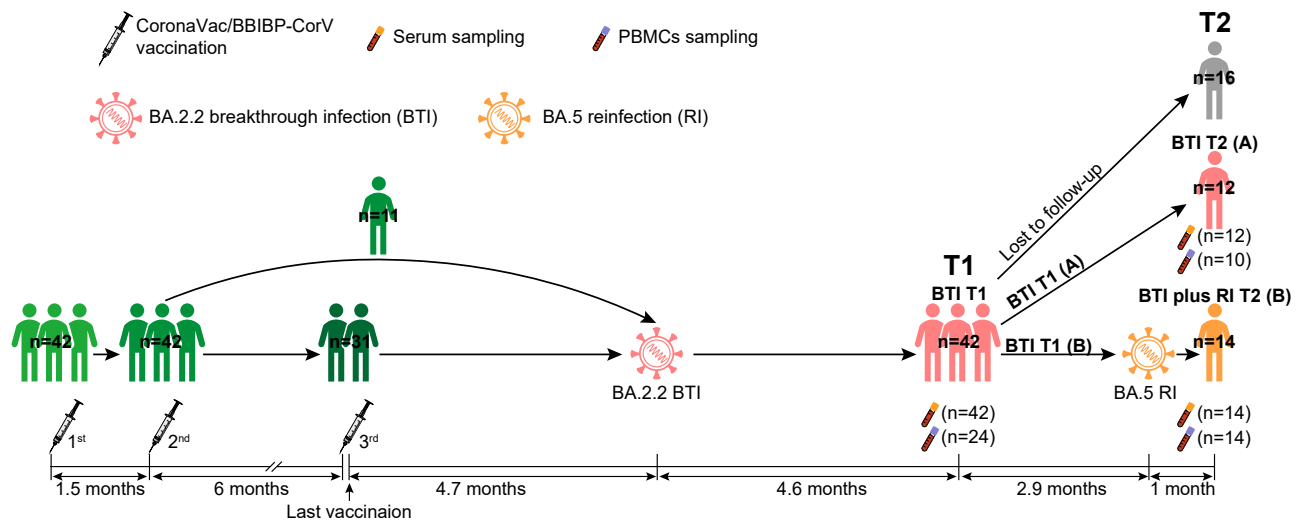


**Figure 1. Study design, participants enrollment, and sampling**

Forty-two participants who immunized with two ( $n = 11$ ) or three ( $n = 31$ ) inactivated vaccines and then suffered Omicron BA.2.2 breakthrough infection (BTI) were enrolled in this study. T1, the first visited time point. T2, the second visited time point. Twelve participants in BTI T2 (A) group and fourteen participants in BTI plus RI T2 (B) group were investigated at T2, while the remained sixteen participants were lost to follow-up at T2. The “n” in the figure represents number of enrolled participants.

CH.1.1, XBB.1.5, XBB.1.16, EG.5.1, and JN.1, respectively. In BTI plus RI T2 (B) group, the NAb titers against Omicron BA.2, BA.5, and BF.7 that were 0.7–1.2 times lower than those against D614G, while the NAb titers against other six Omicron variants that were 6.1–21.9 times lower than those against D614G. All the participants had detectable NAb against D614G, BA.2, BA.5, and BF.7, and over 85% participants also had detectable NAb against other seven Omicron subvariants in BTI plus RI T2 (B) group. Antigenic analysis showed that the relative distance was shorter in BTI plus RI T2 group than that in BTI T1 group, revealing that the SARS-CoV-2 reinfection may alleviate the WT-vaccination induced immune imprinting (Figure S3). Then we compared the NAb titers against the same SARS-CoV-2 strain among five different groups: VacHC, BTI T1 (A), BTI T2 (A), BTI T1 (B), and BTI plus RI T2 (B) (Figure 3B). We found that the NAb titers against D614G and various Omicron subvariants slightly reduced but remained stable in BTI T2 (A) group than those in BTI T1 (A) group except for that against XBB.1.16. Differently, the NAb titers significantly increased in BTI plus RI T2 (B) group compared to those in BTI T1 (B) group. Importantly, the NAb titers against Omicron BA.2, BA.5, and BF.7 were significantly lower in BTI T1 (B) group than those in BTI T1 (A) group, revealing that the level of NAb titers were correlated with subsequently Omicron BA.5 reinfection.

To confirm the results performed by pVNT, we also conducted live virus neutralizing test (LVNT) against SARS-CoV-2 WT strain and Omicron BA.2, BA.5, XBB.1.16 subvariants. Similarly, the NAb titers against Omicron BA.2 and BA.5 were comparable or slightly reduced than those against WT, while the NAb titers against XBB.1.16 were apparently decreased than those against WT (Figure 3C). Also, further comparison among different groups showed that the NAb titers decreased in BTI T2 (A) group compared to BTI T1 (A) group and increased in BTI plus RI T2 (B) group compared to BTI T1 (B) group (Figure 3D). Besides, participants in BTI T1 (B) group had significant lower NAb titers against Omicron BA.5 than those in BTI T1 (A) group, reconfirming that participants with lower NAb titers were more likely to experience SARS-CoV-2 reinfection (Figure 3D).

In addition, no significant difference of vaccination rate upon different doses was observed between BTI T1 (A) and BTI T1 (B) group, revealing that the previous booster vaccination of inactivated WT-vaccines has little effect on the subsequently Omicron BA.5 reinfection (Table S2). What’s more, further comparison of NAb titers between groups by different vaccination background at T1 showed that Omicron BA.2.2 BTI can eliminate the effect of 2- or 3-dose CoronaVac/BBIBP-CorV vaccination on antibody responses (Figures S4A and S4B).

### Well cross-recognized T cell responses after Omicron BTI and reinfection for both Omicron BA.2 and CH.1.1

Then virus-specific T cell responses against Omicron BA.2- and CH.1.1-spike mega peptide pools (MPs) among different groups were evaluated by activation-induced marker (AIM) assays with cytokine intracellular staining (ICS) assays (Figure S5 and Table S3).

Spike-specific CD4<sup>+</sup> and CD8<sup>+</sup> T cell responses against Omicron BA.2 and CH.1.1 MPs were measured by AIM OX40<sup>+</sup>CD137<sup>+</sup> (CD4<sup>+</sup> T cells) or CD69<sup>+</sup>CD137<sup>+</sup> (CD8<sup>+</sup> T cells) (Figures 4A and 4C). For AIM<sup>+</sup>CD4<sup>+</sup> T cells, comparable percentages against Omicron BA.2 and CH.1.1 MPs were observed in T1 group (0.26% and 0.30%) and T2 group (0.27% and 0.26%), respectively. What’s more, there were no significant difference of AIM<sup>+</sup>CD4<sup>+</sup> T cell responses between T1 and T2 group (Figure 4B). Similarly, for AIM<sup>+</sup>CD8<sup>+</sup> T cells, the responses against Omicron BA.2 and CH.1.1 were also comparable in T1 group (0.27% and 0.28%) and T2 group (0.25% and 0.27%), respectively, and the responses against the same peptide between T1 and T2 group were also comparable (Figure 4D). Further comparison showed that there

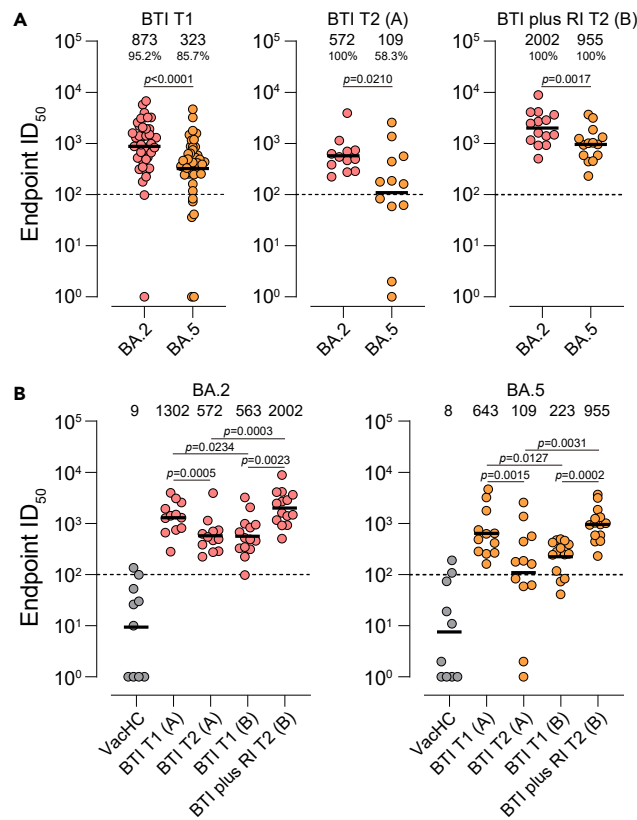


**Figure 2. Omicron BA.2 and BA.5 spike-specific binding IgG antibody responses of the participants at 4- and 8-month post Omicron BA.2.2 breakthrough infection (BTI) with or without subsequent Omicron BA.5 reinfection (RI)**

(A) Dynamic changes of spike-specific binding IgG antibodies against Omicron BA.2 and BA.5 in BTI T1, BTI T2 (A), BTI plus RI T2 (B) group, respectively. (B) Comparison of spike-specific binding IgG antibody titers among groups of BTI T1 (A), BTI T2(A), BTI T1 (B), and BTI plus RI T2 (B). Ten vaccinated participants without infection were selected as healthy controls (VachC) in (B). Geometric mean and detectable prevalence or geometric mean alone is shown at the top of each panel. The black dashed line indicates the threshold for initial dilution (1:100). Wilcoxon matched-pairs signed rank test was performed in (A). Wilcoxon matched-pairs signed rank test and Mann-Whitney test were performed in (B).  $P$  values  $< 0.05$  was considered statistically significant.

was no significant difference of AIM<sup>+</sup>CD4<sup>+</sup> or CD8<sup>+</sup> T cell responses between groups of BTI T1 (A), BTI T2 (A), BTI T1 (B), and BTI plus RI T2 (B) by different Omicron spike MPs (Figures S6A and S6B).

Then the spike-specific CD4<sup>+</sup> or CD8<sup>+</sup> T cells secreting TNF- $\alpha$ , IL-2, and IFN- $\gamma$  were measured by ICS assays (Figures 5A and 5C). Regardless of different visited time points, the percentage of spike-specific TNF- $\alpha$ <sup>+</sup>, IL-2<sup>+</sup>, and IFN- $\gamma$ <sup>+</sup> of CD4<sup>+</sup> or CD8<sup>+</sup> T cells was comparable when stimulated by Omicron BA.2 or CH.1.1 MPs (Figures 5B and 5D). Considering the reinfection status, at the same time point, we found that the ICS CD4<sup>+</sup> or CD8<sup>+</sup> T cell responses detected after restimulation with Omicron BA.2 or CH.1.1 MPs were similar without significant difference (Figures S7A and S7B). However, the TNF- $\alpha$ <sup>+</sup> CD8<sup>+</sup> T cell responses detected after restimulation with both BA.2 and CH.1.1 were significantly higher in BTI plus RI T2 (B) group than that in BTI T2 (A) group (Figures S7A and S7B). We further analyzed the polyfunctional profiles of T cells in participants and demonstrate similar capacities for cytokines co-expression for both Omicron BA.2 and CH.1.1-specific T cells at T1 or T2, indicating the normal function in cross-reactive Omicron T cell responses (Figures 5E–5H). Notably, there were also no differences in the polyfunctional profiles between T1 and T2 for either ICS CD4<sup>+</sup> or CD8<sup>+</sup> T cells, suggesting that the ICS<sup>+</sup> responses maintained stable after Omicron BA.2.2 BTI (Figures 5E–5H). Considering the reinfection status, no significant differences in the polyfunctional profiles were found among groups of BTI T1 (A), BTI T1 (B), BTI T2 (A), and BTI plus RI T2 (B) for either CD4<sup>+</sup> or CD8<sup>+</sup> T cells (Figures S7C and S7D).

### Omicron BA.5 reinfection can promote the differentiation of virus-specific CD8<sup>+</sup> T cells

To explore the differentiation patterns of Omicron BA.2 and CH.1.1 spike-specific memory T cells at different visited time points, surface markers of CD45RA and CCR7 were selected to subdivide spike-specific memory T cells into central memory T cells (TCM, CD45RA<sup>-</sup>CCR7<sup>+</sup>), naive T cells (Tnaive, CD45RA<sup>+</sup>CCR7<sup>+</sup>), effector memory T cells (TEM, CD45RA<sup>-</sup>CCR7<sup>-</sup>) and terminally differentiated effector memory T cells (TEMRA, CD45RA<sup>+</sup>CCR7<sup>-</sup>) by detecting expressions on virus-specific IFN- $\gamma$ <sup>+</sup> T cells (Figure 6A). The results showed that Tnaive and TEM were the two main subsets of Omicron BA.2 and CH.1.1 spike-specific CD4<sup>+</sup> T cells, and there was no

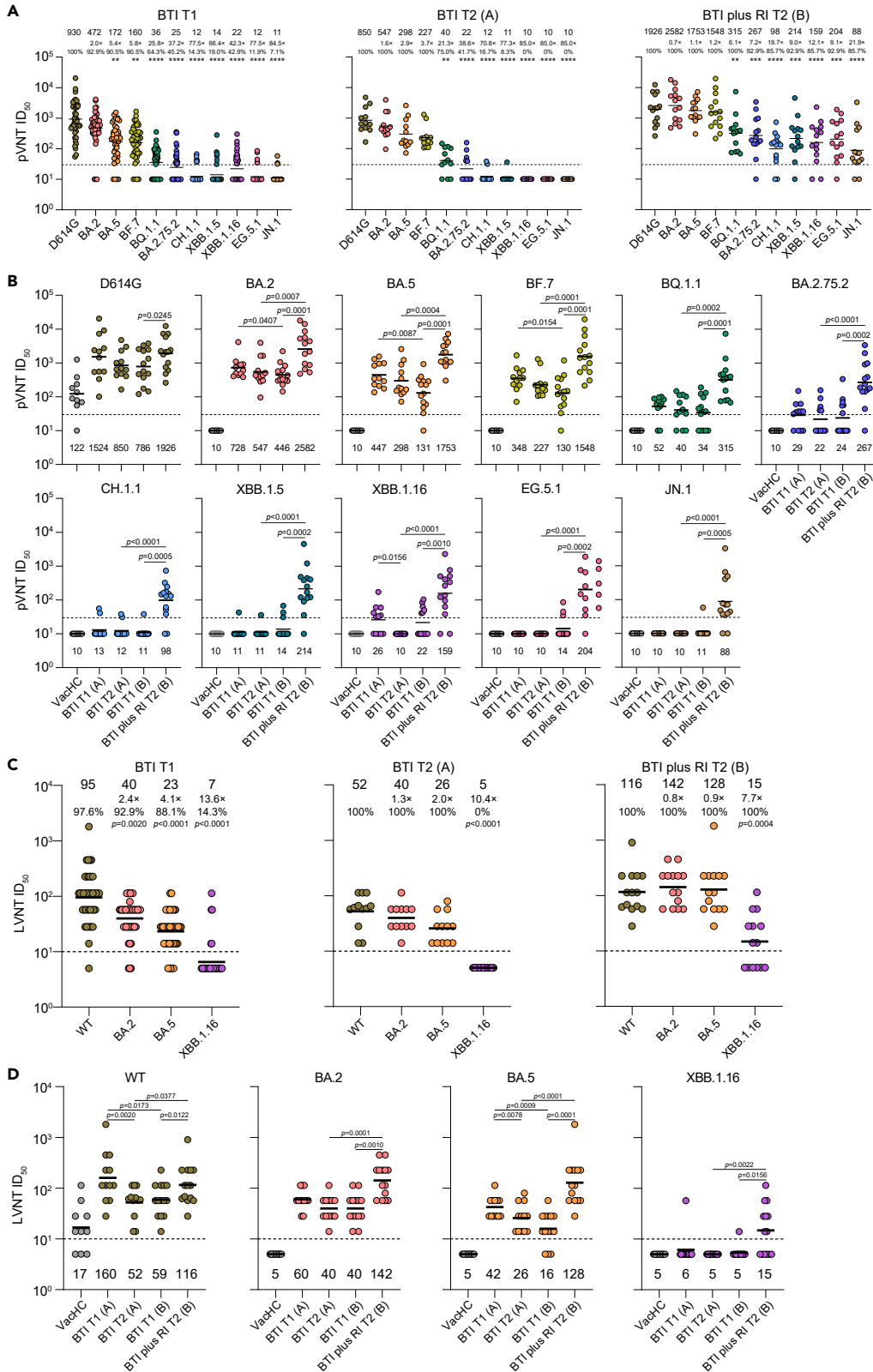


**Figure 3. Neutralizing antibody titers by pseudovirus neutralization test (pVNT) and live-virus neutralization test (LVNT) against D614G and emerging Omicron subvariants of the participants at 4-, and 8-month post Omicron BA.2.2 breakthrough infection (BTI) with or without subsequent Omicron BA.5 reinfection (RI)**

(A) Dynamic changes of neutralizing antibody titers against D614G and Omicron BA.2, BA.5, BF.7, BQ.1.1, BA.2.75.2, CH.1.1, XBB.1.5, XBB.1.16, EG.5.1, and JN.1 in BTI T1, BTI T2 (A), BTI plus RI T2 (B) group, respectively.  
 (B) Comparison of virus-specific neutralizing antibody titers among D614G and various emerging Omicron subvariants among groups of BTI T1 (A), BTI T2(A), BTI T1 (B), and BTI plus RI T2 (B).  
 (C) Dynamic changes of neutralizing antibody titers against Wild-type (WT) and Omicron BA.2, BA.5, and XBB.1.16 in BTI T1, BTI T2 (A), BTI plus RI T2 (B) group, respectively.  
 (D) Comparison of virus-specific neutralizing antibody titers among WT and various emerging Omicron subvariants among groups of BTI T1 (A), BTI T2 (A), BTI T1 (B), and BTI plus RI T2 (B). Ten vaccinated participants without infection were selected as healthy controls (VacHC) in (B and D). Values of GMT with reduction times compared to D614G, and the prevalence of detectable NAb titers above 30 were shown in the (A). Values of GMT were shown at the bottom of (B and D). Values of GMT with reduction times compared to WT, and the prevalence of detectable NAb titers above 10 were shown in the (C). The black dashed line indicates the threshold for detectable NAb titers ( $ID_{50} = 30$ ) in (A and B). The black dashed line indicates the threshold for detectable NAb titers ( $ID_{50} = 10$ ) in (C and D). The spacing of the grid lines in (C) corresponds to the neutralizing antibody titers unit, which was equivalent to the 2-fold change in the neutralizing  $ID_{50}$  titer. Friedman test was performed in (A and C). Wilcoxon matched-pairs signed rank test and Mann-Whitney test were performed in (B and D).  $P$  values  $<0.05$  was considered statistically significant. The asterisk in (A) indicates the significant difference between D614G and each of the Omicron subvariant. The  $p$  value in (C) represents the difference between WT and each of Omicron subvariant.  $**p < 0.01$ ,  $***p < 0.001$ ,  $****p < 0.0001$ .

significant difference for subsets by different stimulated MPs or visited time points (Figure 6B). Regarding virus spike-specific  $CD8^+$  T cells, the TEMRA was the main subset, and its percentage was significantly reduced at T2 compared to that at T1 for Omicron BA.2 (Figure 6C).

Considering the reinfection status, we found that the changes of phenotypic differentiation of spike-specific memory  $CD4^+$  T cells were not apparently affected by reinfection status (Figures S8A and S8B). For spike-specific memory  $CD8^+$  T cells, the Tnaive subset was slightly or significantly reduced in BTI plus RI T2 (B) group compared to BTI T1 (B) group, while the Tnaive subset was slightly higher in BTI T2 (A) group than that in BTI T1 (A) group (Figures S8C and S8D). Further comparison between group A and B at the same time points showed that the subjects in BTI plus RI T2 (B) group had higher percentage of TEM and lower percentage of Tnaive than those in BTI T2 (A) group for virus spike-specific  $CD8^+$  T cells (Figures S8E–S8H).

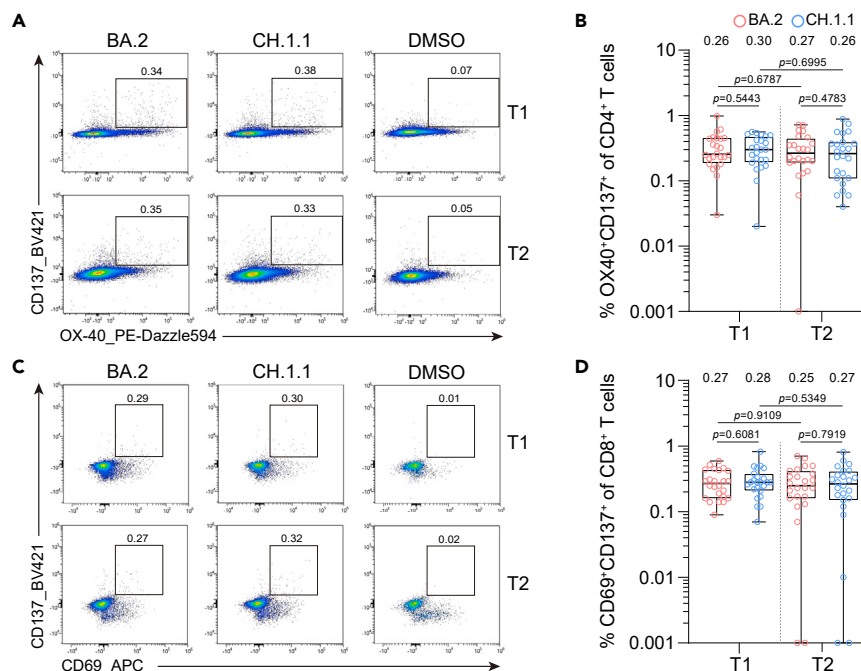


**Figure 4. Omicron BA.2 and CH.1.1-specific  $AIM^+CD4^+$  or  $AIM^+CD8^+$  T cell responses in participants at 4- and 8-month post Omicron BA.2.2 breakthrough infection (BTI) with or without Omicron BA.5 reinfection (RI)**

The percentage of  $AIM^+$  ( $OX40^+CD137^+$ ) of  $CD4^+$  T cells (A and B) and  $AIM^+$  ( $CD69^+CD137^+$ ) of  $CD8^+$  T cells (C and D) after stimulation of PBMCs with Omicron BA.2 or CH.1.1 spike-specific MPs. Data showed above (B and D) represent the median of percentage. Graphs show individual response of  $AIM^+$   $CD4^+$  or  $CD8^+$  T cell responses against Omicron BA.2 or CH.1.1 MPs plotted as background subtracted DMSO negative controls. Boxplots indicate median and interquartile range (IQR). Wilcoxon matched-pairs signed rank test was performed in (B and D), and  $p$  values  $<0.05$  was considered statistically significant.



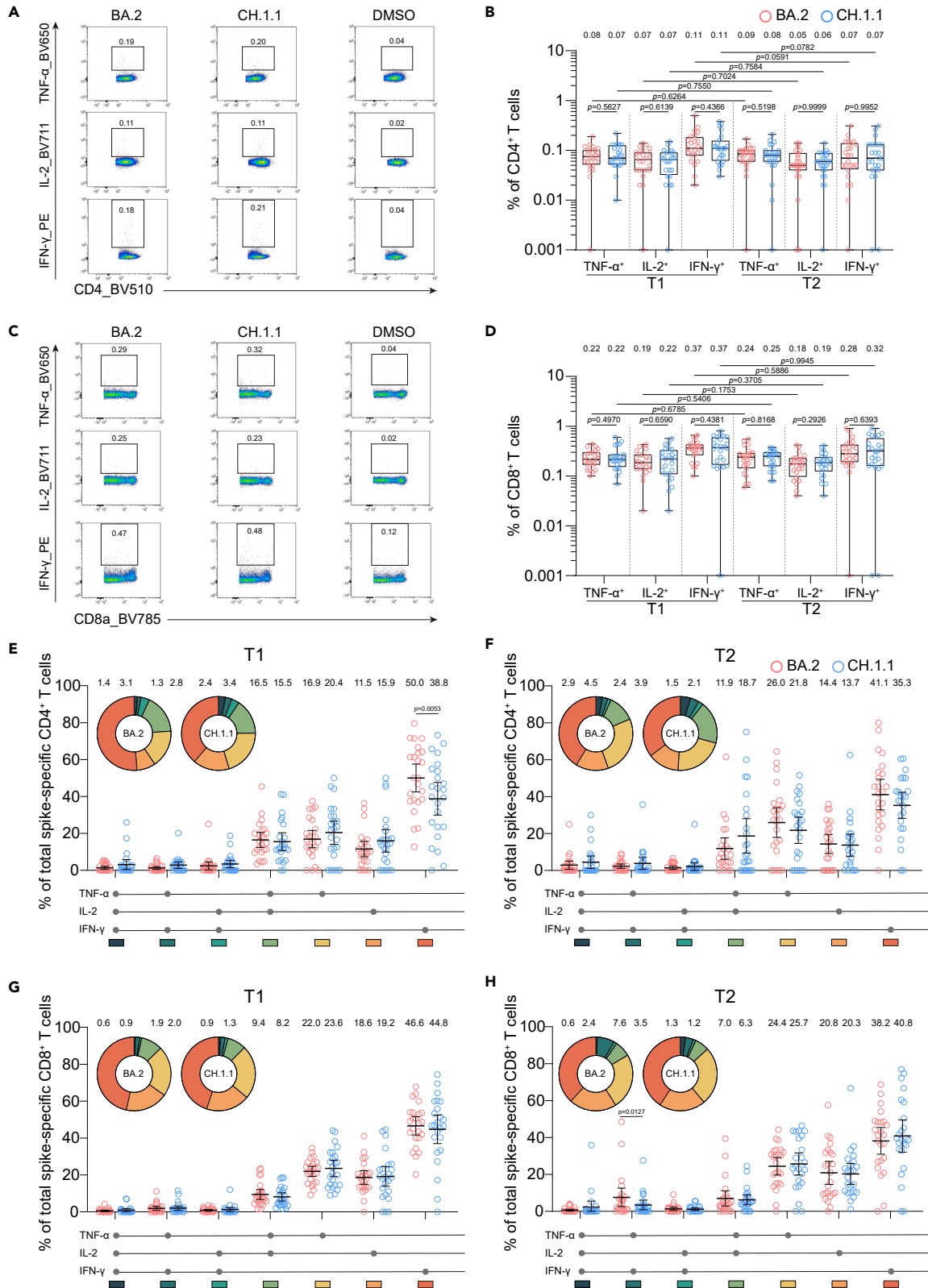


**Figure 5. Spike-specific ICS<sup>+</sup> CD4<sup>+</sup> or CD8<sup>+</sup> T cell responses against Omicron BA.2 or CH.1.1 in participants at 4- and 8-month post Omicron BA.2.2 breakthrough infection (BTI) with or without Omicron BA.5 reinfection (RI)**

The percentage of TNF- $\alpha$ <sup>+</sup>, IL-2<sup>+</sup>, and IFN- $\gamma$ <sup>+</sup> for CD4<sup>+</sup> T cells (A and B) and the percentage of TNF- $\alpha$ <sup>+</sup>, IL-2<sup>+</sup>, and IFN- $\gamma$ <sup>+</sup> for CD8<sup>+</sup> T cells (C and D) after stimulation of PBMCs with Omicron BA.2 or CH.1.1 spike-specific MPs. Comparison of the polyfunctional profile between Omicron BA.2 and CH.1.1 spike-specific CD4<sup>+</sup> T cells (E and G) or CD8<sup>+</sup> T cells (F and H) at 4-month and 8-month. Data showed above (B and D–H) represent median and mean, respectively. Graphs show individual response of ICS<sup>+</sup> CD4<sup>+</sup> or CD8<sup>+</sup> T cell responses against Omicron BA.2 or CH.1.1 MPs plotted as background subtracted DMSO negative controls. Boxplots indicate median and interquartile range (IQR). Bars indicate Mean with 95% confidence interval in (E–H). Each response pattern (i.e., any possible combination of IFN- $\gamma$ , IL-2 or TNF- $\alpha$  expression) is color-coded, and data are summarized in the pie charts in (E–H). No significant differences were observed between pies using a permutation test for ICS<sup>+</sup> CD4<sup>+</sup> or ICS<sup>+</sup> CD8<sup>+</sup> T cell responses. Wilcoxon matched-pairs signed rank test was performed in (B and D–H), and *p* values <0.05 was considered statistically significant.

### Omicron BA.5 reinfection can enhance the correlation among parameters of antibody responses

To explore whether correlations exist between antibody and T cell responses, we correlated the measured immune parameters including binding IgG antibody, pVNT-NAb, LVNT-NAb, and T cell responses among different groups (Figures 7A–7F, Table S4). Overall, the correlation among different parameters was apparently strengthened at T2 compared to T1, especially for the correlation among the parameters defining antibody responses (Figures 7A and 7B). Considering the reinfection status, strong correlations among antibody parameters were observed in BTI plus RI T2 (B) group than that in BTI T2 (A) group (Figures 7C–7F). Of note, the correlation between antibodies and T cells had a high proportion of inverse correlations, regardless of visited time points and reinfection status.

### DISCUSSION

In this study, we conducted a longitudinal study to investigate the persistence of humoral and cellular immunity among 42 participants with two followed-up time points (4- and 8-month) post Omicron BA.2.2 BTI with or without Omicron BA.5 reinfection. We found that the IgG and

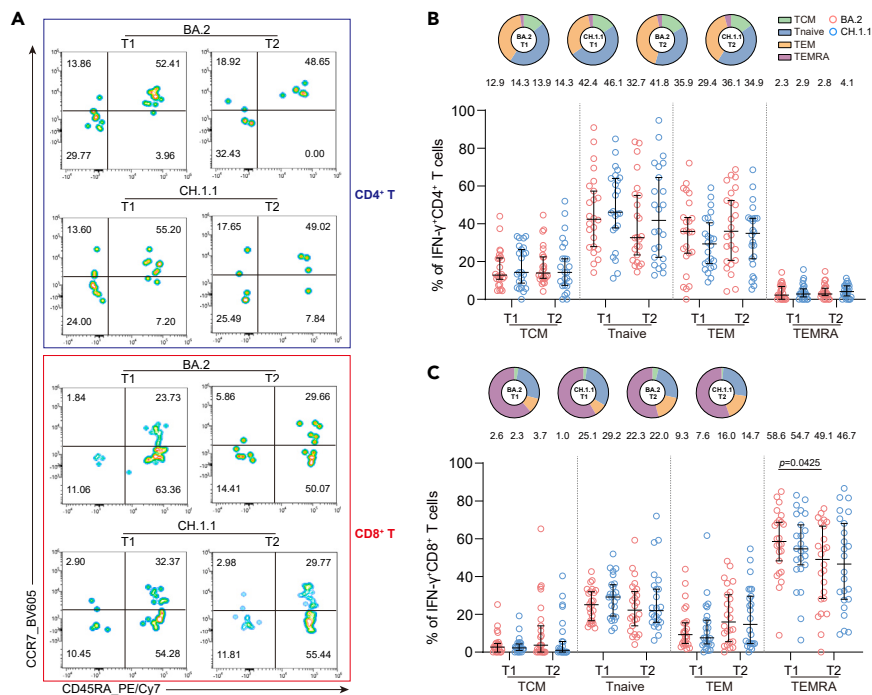


**Figure 6. Memory phenotype differentiation of Omicron BA.2- or CH.1.1-specific memory T cells in participants at 4- and 8-month post Omicron BA.2.2 BTI with or without Omicron BA.5 reinfection**

(A) Flow cytometry plots in Omicron BA.2 and CH.1.1 MPs stimulated groups showing spike-specific memory CD4<sup>+</sup> and CD8<sup>+</sup> T cell phenotypes in ex vivo assay. Data showed in (A) represents the percentages for different subsets.

Frequency of different spike-specific memory CD4<sup>+</sup> T cell (B) and CD8<sup>+</sup> T cell (C) phenotypes in Omicron BA.2 and CH.1.1 groups at 4-month and 8-month post BA.2 BTI. Data showed above (B and C) represent median of percentage. Bars indicate median with 95% confidence interval (CI). Each subset of memory phenotype differentiation is color-coded, and data are summarized in the pie charts in (B and C). No significant differences were observed between pies using a permutation test in each panel. Wilcoxon matched-pairs signed rank test was performed in (B and C), and *p* values <0.05 was considered statistically significant.

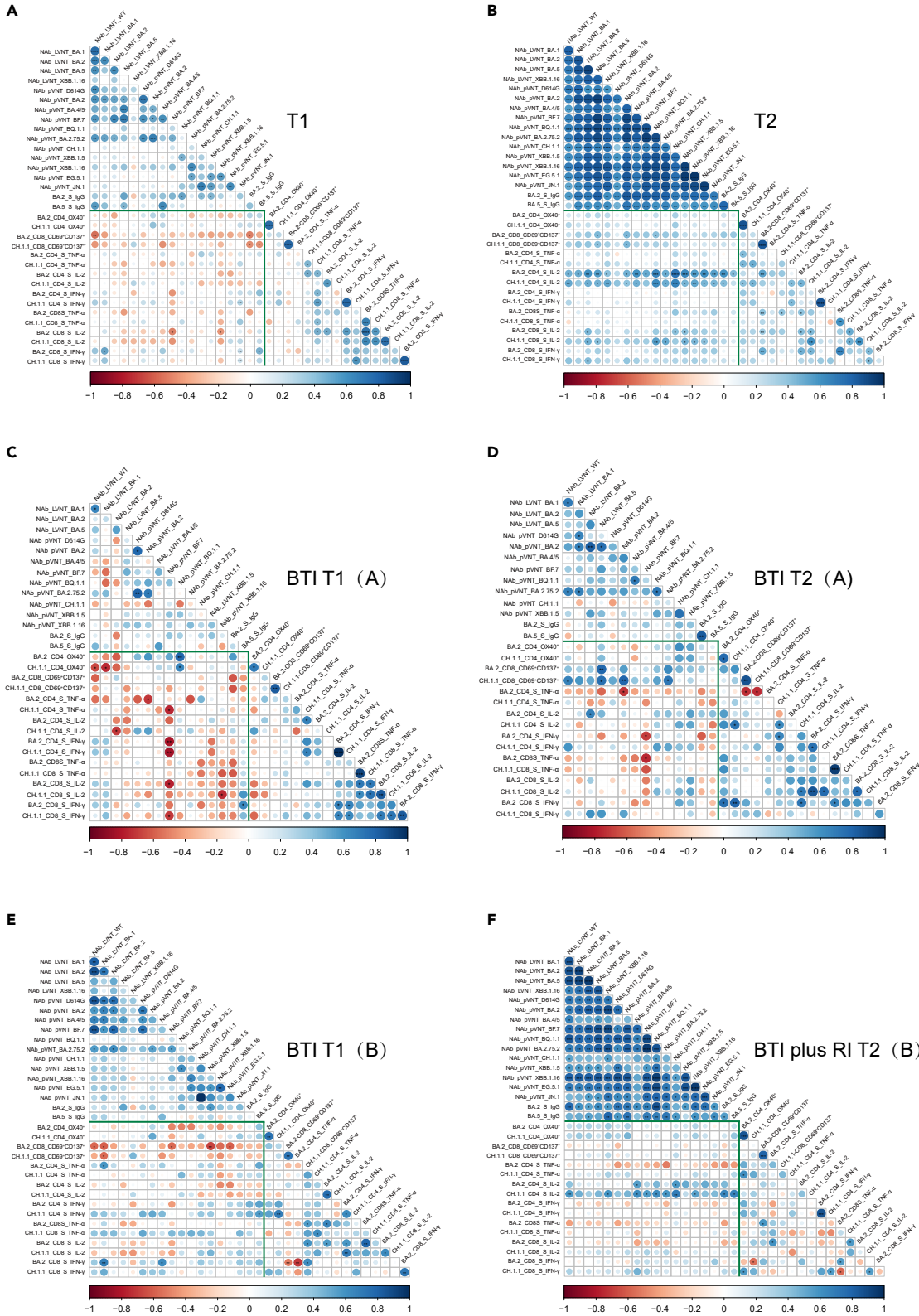


**Figure 7. Correlation between the parameters of the adaptive immune response at 4-, and 8-month post Omicron BA.2.2 BTI with or without Omicron BA.5 reinfection**

Correlation between the parameters at 4-month (A), and 8-month (B). Correlation between the parameters for participants without subsequent Omicron BA.5 reinfection at 4-month (C) and 8-month (D). Correlation between the parameters for participants with subsequent Omicron BA.5 reinfection at 4-month (E) and 8-month (F). The strength of correlations was assessed by the two-side Spearman's correlation test. Correlation strength is shown by the size and color of the circle and statistical significance is shown by asterisks. \* $p < 0.05$ , \*\* $p < 0.01$ , \*\*\* $p < 0.001$ , \*\*\*\* $p < 0.0001$ . The exact  $r$  and  $p$  values are given in the Table S4. Green lines separate correlations between different measured immune parameters (antibody responses and T cell responses).

NAb titers were reduced at 8-month compared to that at 4-month among the participants without Omicron BA.5 reinfection. Nearly all the serum remained detectable NAb titers against the previous Omicron subvariants (BA.2, BA.5, and BF.7), and partial or all of them lost the neutralization against emerging Omicron subvariants (BQ.1.1, BA.2.75.2, CH.1.1, XBB.1.5, XBB.1.16, EG.5.1, and JN.1). The level of IgG and NAb titers at BTI T1 was correlated with subsequent Omicron BA.5 reinfection, and SARS-CoV-2 reinfection could enhance the neutralizing ability against the emerging Omicron subvariants. Well-recognized immunity was observed for virus-specific T cell responses against different Omicron subvariants MPs. Omicron BA.5 reinfection could enhance the secretion of virus-specific TNF- $\alpha^+$ /IL-2 $^+$ /IFN- $\gamma^+$  T cells and promote the differentiation of virus-specific CD8 $^+$  T cells, but had no significant effect on AIM $^+$  T cell responses.

Previous studies have showed that the subjects with Omicron BA.1, BA.2, or BA.5 subvariants BTI had higher NAb titers than that of vaccinated individuals,<sup>7,9,10</sup> and could well neutralized prior circulating Omicron subvariants (BA.1, BA.2, BA.4, or BA.5) at early convalescent stage.<sup>8-11,13-15</sup> However, only several studies assessed the persistence of humoral immunity against limited representative SARS-CoV-2 variants beyond 6 months post Omicron subvariants BTI.<sup>22,23,35</sup> In this study, we found that the IgG and NAb titers were decreased at 8-month compared to 4-month among participants without Omicron BA.5 reinfection, revealing that the risk of SARS-CoV-2 reinfection increases with the extension of time interval post antigen exposure. Meanwhile, we found that serum from most of the participants had neutralizing ability against D614G, BA.2, BA.5, and BF.7 strains, while those partial or full lost the neutralizing ability against BQ.1.1, BA.2.75.2, CH.1.1, XBB.1.5, XBB.1.16, EG.5.1, and JN.1 subvariants at both 4- and 8-month post Omicron BA.2 BTI, suggesting that the immune escape ability of emerging Omicron subvariants is gradually enhanced. Similar with the previous studies, the Omicron BA.5 reinfection may enhance the neutralizing ability and alleviate WT-vaccination induced immune imprinting.<sup>36</sup> Besides, the level of IgG and NAb after Omicron BA.2 BTI was correlated with subsequent Omicron BA.5 infection, clarifying the important role of humoral immunity in preventing infection.<sup>37,38</sup>

Clearly, humoral immunity plays a critical role in viral neutralization, but there is evidence that the virus may spread by cell-to-cell contact which is resistant to NAb neutralization,<sup>39</sup> suggesting that T cell responses may be important for viral clearance and prevention of infection.<sup>28,29,40</sup> Previous studies have shown that T cell responses can well cross-recognize the SARS-CoV-2 WT and Omicron BA.1 strains.<sup>30,31,41</sup> In this study, in view of the previous strain of infection and the circulating variants at that time, we selected the Omicron BA.2 and CH.1.1 subvariants to synthesize the corresponding MPs against the spike gene, in which thirteen amino acid differences exist between the two Omicron subvariants in the spike that affect about 10% (25/252) of peptide sequences. Based on those previous studies, we further clarified the well cross-recognition of T cell responses between Omicron BA.2 and CH.1.1 strains post Omicron BA.2.2 BTI and Omicron BA.5 reinfection, implying that T cell responses may play a vital role in preventing emerging SARS-CoV-2 variants, especially for those with strong escape ability against NAb neutralization.

Given the reinfection status, we found that the ICS $^+$  CD4 $^+$  or CD8 $^+$  responses were slightly or significantly higher in BTI plus RI T2 (B) group than those in BTI T2 (A) group, indicating that antigen exposure can promote the secretion of TNF- $\alpha^+$ , IL-2 $^+$ , and IFN- $\gamma^+$  by virus-specific CD4 $^+$  or CD8 $^+$  T cells.<sup>42,43</sup> However, the ICS $^+$  T cell responses were comparable between BTI plus RI T2 (B) group and BTI T1 (B) group, without the expected increase after SARS-CoV-2 reinfection. Combined with the recent studies of T cell responses in acute stage,<sup>44,45</sup> we speculate that virus-specific CD4 $^+$  or CD8 $^+$  T cells are robustly activated within the first week and then reduced quickly over one month after antigen exposure.

Consistent with the previous studies,<sup>41,46</sup> Tnaive is the main phenotypic subset of virus-specific CD4 $^+$  T cells, while TEMRA is the main phenotypic subset for virus-specific CD8 $^+$  T cells at 4-month post BA.2.2 BTI. What's more, slightly or significantly changes of Tnaive and TEM subsets were observed in BTI plus RI T2 (B) group compared to BTI T2 (A) and BTI T1 (B) group, revealing that the differentiation changes from Tnaive to TEM after reinfection may play an important role in preventing severe diseases.<sup>46,47</sup> Obviously, the percentage of asymptomatic patients post Omicron BA.5 reinfection is higher than those post Omicron BA.2.2 BTI in this study.

Similar with the documented study,<sup>48</sup> we also found that additional antigen exposure can strengthen the correlation between detected parameters defining the adaptive immune responses, indicating that SARS-CoV-2 reinfection may enhance the body immunity to combat the emerging variants. Surprisingly, inverse correlations possessed higher percentage between humoral and cellular parameters in this study, suggesting that the kinetic changes of the humoral and cellular response are inconsistent after antigen exposure and the correlation between them may more likely be reflected in Tfh cell-mediated response of lymphoid tissues rather than in detected T cell response of peripheral blood.<sup>45,46</sup>

In conclusion, this study has expanded our understanding of immunity persistence and cross-reactivity of T cell response among individuals post Omicron subvariants BTI and reinfection. For one thing, emerging Omicron subvariants extensively escape the immunity elicited by prior Omicron subvariant BTI, while SARS-CoV-2 reinfection can significantly enhance the neutralization and may alleviate the WT-vaccination induced immune imprinting. For another thing, well cross-recognized immunity is still observed between different Omicron subvariants and SARS-CoV-2 reinfection can boost the ICS $^+$  T cell responses and promote the differentiation of CD8 $^+$  T cell subsets. Taken together, our data

support the use of updated vaccines based on the newly identified Omicron subvariants or the conserved T cells to combat the diverse emerging SARS-CoV-2 variants.

### Limitations of the study

Our study has several limitations. Firstly, limited numbers of participants were investigated at 8-month post Omicron BA.2.2 BT1. Secondly, we focused more attention on virus spike-specific immunity and were not able to assess the function of SARS-CoV-2-specific T cells targeting antigens other than spike. Besides, we only got serum and PBMCs at convalescent stages and could not accurately grasp the dynamic changes of humoral and cellular responses. Therefore, more prospective studies with multiple followed-up time points and enough clinical samples are needed to confirm and expand the results in the study.

### STAR★METHODS

Detailed methods are provided in the online version of this paper and include the following:

- [KEY RESOURCES TABLE](#)
- [RESOURCE AVAILABILITY](#)
  - Lead contact
  - Materials availability
  - Data and code availability
- [EXPERIMENTAL MODEL AND STUDY PARTICIPANT DETAILS](#)
  - Study participants
  - Ethics statement
- [METHOD DETAILS](#)
  - Peripheral blood mononuclear cells (PBMCs) isolation
  - Enzyme-linked immunosorbent assay analysis of IgG antibody to spike trimer of Omicron BA.2 and BA.5
  - Production of variant SARS-CoV-2 spike plasmid pseudovirus
  - Pseudovirus neutralization test
  - Live-virus neutralization test
  - Antigenic Cartography
  - SARS-CoV-2 BA.2 and CH.1.1 spike peptide synthesis and pooling
  - Flow cytometry-based T cell assays
- [QUANTIFICATION AND STATISTICAL ANALYSIS](#)

### SUPPLEMENTAL INFORMATION

Supplemental information can be found online at <https://doi.org/10.1016/j.isci.2024.110283>.

### ACKNOWLEDGMENTS

We thank all subjects for their participation and for providing their blood for this study. This study was supported by Beijing Natural Science Foundation (L222119 to Guo-Lin Wang), the National Natural Science Foundation of China (82103901 to Guo-Lin Wang), the China Mega-Project on Infectious Disease Prevention (2021YFC2302004 to Bao-Gui Jiang), and the State Key Laboratory of Pathogen and Biosecurity (SKLPBS2205 to Chen-Long Lv).

### AUTHOR CONTRIBUTIONS

Conceptualization, L.Q.F., G.L.W., X.L., and H.W.; data curation, G.L.W. and L.Q.F.; methodology, G.L.W., X.J.Z., C.S., D.Y.L., S.Z., H.J.G., C.L.Z., and H.W.; formal analysis, X.J.Z., G.L.W., C.S., D.Y.L., J.J.C., Q.X., C.L.L., and B.G.J.; investigation, B.J., H.H.P., C.Q., C.S., and Y.S.; funding acquisition, G.L.W., B.G.J., and C.L.L.; writing, G.L.W., L.Q.F., X.J.Z., and B.J.; supervision, L.Q.F., G.L.W., Z.Q.K., and H.W.

### DECLARATION OF INTERESTS

The authors declare no competing interests.

Received: December 11, 2023

Revised: April 23, 2024

Accepted: June 13, 2024

Published: June 15, 2024

## REFERENCES

1. Qu, P., Evans, J.P., Faraone, J.N., Zheng, Y.M., Carlin, C., Anghelina, M., Stevens, P., Fernandez, S., Jones, D., Lozanski, G., et al. (2023). Enhanced neutralization resistance of SARS-CoV-2 Omicron subvariants BQ.1, BQ.1.1, BA.4.6, BF.7, and BA.2.75.2. *Cell Host Microbe* 31, 9–17.e3. <https://doi.org/10.1016/j.chom.2022.11.012>.
2. Qu, P., Faraone, J.N., Evans, J.P., Zheng, Y.M., Carlin, C., Anghelina, M., Stevens, P., Fernandez, S., Jones, D., Panchal, A.R., et al. (2023). Enhanced evasion of neutralizing antibody response by Omicron XBB.1.5, CH.1.1, and CA.3.1 variants. *Cell Rep.* 42, 112443. <https://doi.org/10.1016/j.celrep.2023.112443>.
3. Yamasoba, D., Uriu, K., Plianchaisuk, A., Kosugi, Y., Pan, L., Zahradnik, J., Genotype to Phenotype Japan G2P-Japan Consortium, Ito, J., and Sato, K. (2023). Viriologic characteristics of the SARS-CoV-2 omicron XBB.1.16 variant. *Lancet Infect. Dis.* 23, 655–656. [https://doi.org/10.1016/S1473-3099\(23\)00278-5](https://doi.org/10.1016/S1473-3099(23)00278-5).
4. Faraone, J.N., Qu, P., Goodarzi, N., Zheng, Y.-M., Carlin, C., Saif, L.J., Oltz, E.M., Xu, K., Jones, D., Gumina, R.J., and Liu, S.-L. (2023). Immune Evasion and Membrane Fusion of SARS-CoV-2 XBB Subvariants EG.5.1 and XBB.2.3. Preprint at bioRxiv. <https://doi.org/10.1101/2023.08.30.555188>.
5. Uriu, K., Ito, J., Kosugi, Y., Tanaka, Y.L., Mugita, Y., Guo, Z., Hinay, A.A., Jr., Putri, O., Kim, Y., Shimizu, R., et al. (2023). Transmissibility, infectivity, and immune evasion of the SARS-CoV-2 BA.2.86 variant. *Lancet Infect. Dis.* 23, e460–e461. [https://doi.org/10.1016/S1473-3099\(23\)00575-3](https://doi.org/10.1016/S1473-3099(23)00575-3).
6. Yang, S., Yu, Y., Xu, Y., Jjian, F., Song, W., Yisimayi, A., Wang, P., Wang, J., Liu, J., Yu, L., et al. (2024). Fast evolution of SARS-CoV-2 BA.2.86 to JN.1 under heavy immune pressure. *Lancet Infect. Dis.* 24, e70–e72. [https://doi.org/10.1016/S1473-3099\(23\)00744-2](https://doi.org/10.1016/S1473-3099(23)00744-2).
7. Xie, X., Zou, J., Kurhade, C., Liu, M., Ren, P., and Pei-Yong, S. (2022). Neutralization of SARS-CoV-2 Omicron sublineages by 4 doses of the original mRNA vaccine. *Cell Rep.* 41, 111729. <https://doi.org/10.1016/j.celrep.2022.111729>.
8. Ju, B., Fan, Q., Wang, M., Liao, X., Guo, H., Wang, H., Ge, X., Liu, L., and Zhang, Z. (2022). Antigenic sin of wild-type SARS-CoV-2 vaccine shapes poor cross-neutralization of BA.4/5/2.75 subvariants in BA.2 breakthrough infections. *Nat. Commun.* 13, 7120. <https://doi.org/10.1038/s41467-022-34400-8>.
9. Atari, N., Kliker, L., Zuckerman, N., Elkader, B.A., Weiss-Ottolenghi, Y., Mendelson, E., Kreiss, Y., Regev-Yochay, G., and Mandelboim, M. (2022). Omicron BA.2.75 variant is efficiently neutralised following BA.1 and BA.5 breakthrough infection in vaccinated individuals, Israel, June to September 2022. *Euro Surveill.* 27, 2200785. <https://doi.org/10.2807/1560-7917.ES.2022.27.44.2200785>.
10. Cheng, S.S., Mok, C.K., Li, J.K., Ng, S.S., Lam, B.H., Jeevan, T., Kandail, A., Pekosz, A., Chan, K.C., Tsang, L.C., et al. (2022). Plaque-neutralizing antibody to BA.2.12.1, BA.4 and BA.5 in individuals with three doses of BioNTech or CoronaVac vaccines, natural infection and breakthrough infection. *J. Clin. Virol.* 156, 105273. <https://doi.org/10.1016/j.jcv.2022.105273>.
11. Brazer, N., Morris, M.K., Servellita, V., Anglin, K., Saldhi, P., Garcia-Knight, M., Bethancourt, S., Sotomayor-Gonzalez, A., Wang, B., Foresythe, A., et al. (2022). Neutralizing Immunity Induced Against the Omicron BA.1 and BA.2 Variants in Vaccine Breakthrough Infections. *J. Infect. Dis.* 226, 1688–1698. <https://doi.org/10.1093/infdis/jiac384>.
12. Karaba, A.H., Johnston, T.S., Aytenfisu, T.Y., Woldemeskel, B.A., Garliss, C.C., Cox, A.L., and Blankson, J.N. (2022). Low neutralisation of the omicron BA.2 sublineage in boosted individuals who had breakthrough infections. *Lancet Microbe* 3, e644. [https://doi.org/10.1016/S2666-5247\(22\)00180-X](https://doi.org/10.1016/S2666-5247(22)00180-X).
13. Wang, Q., Guo, Y., Iketani, S., Nair, M.S., Li, Z., Mohri, H., Wang, M., Yu, J., Bowen, A.D., Chang, J.Y., et al. (2022). Antibody evasion by SARS-CoV-2 Omicron subvariants BA.2.12.1, BA.4 and BA.5. *Nature* 608, 603–608. <https://doi.org/10.1038/s41586-022-05053-w>.
14. Muik, A., Lui, B.G., Bacher, M., Wallisch, A.K., Toker, A., Finlayson, A., Krüger, K., Ozhelvaci, O., Grikscheit, K., Hoehl, S., et al. (2022). Omicron BA.2 breakthrough infection enhances cross-neutralization of BA.2.12.1 and BA.4/BA.5. *Sci. Immunol.* 7, eade2283. <https://doi.org/10.1126/sciimmunol.ade2283>.
15. Yang, Y., Gong, X., Wang, J., Fang, S., Zhang, J., Liao, X., Guan, Y., Wu, W., Liu, Y., and Lu, H. (2022). Comparative neutralization profiles of naive and breakthrough infections with Delta, Omicron BA.1 and BA.2 variants of SARS-CoV-2. *Signal Transduct. Targeted Ther.* 7, 316. <https://doi.org/10.1038/s41392-022-01166-w>.
16. Lee, W.S., Tan, H.X., Reynaldi, A., Esterbauer, R., Koutsakos, M., Nguyen, J., Amarasena, T., Kent, H.E., Aggarwal, A., Turville, S.G., et al. (2023). Durable reprogramming of neutralizing antibody responses following Omicron breakthrough infection. *Sci. Adv.* 9, eadg5301. <https://doi.org/10.1126/sciadv.adg5301>.
17. Yisimayi, A., Song, W., Wang, J., Jian, F., Yu, Y., Chen, X., Xu, Y., Yang, S., Niu, X., Xiao, T., et al. (2023). Repeated Omicron infection alleviates SARS-CoV-2 immune imprinting. Preprint at bioRxiv. <https://doi.org/10.1101/2023.05.01.538516>.
18. Jeong, H.W., Kim, S.M., Jung, M.K., Noh, J.Y., Yoo, J.S., Kim, E.H., Kim, Y.I., Yu, K., Jang, S.G., Gil, J., et al. (2022). Enhanced antibody responses in fully vaccinated individuals against pan-SARS-CoV-2 variants following Omicron breakthrough infection. *Cell Rep. Med.* 3, 100764. <https://doi.org/10.1016/j.xcrm.2022.100764>.
19. Pedersen, R.M., Bang, L.L., Tornby, D.S., Madsen, L.W., Holm, D.K., Sydenham, T.V., Johansen, I.S., Jensen, T.G., Justesen, U.S., and Andersen, T.E. (2022). Omicron BA.5 Neutralization among Vaccine-Boosted Persons with Prior Omicron BA.1/BA.2 Infections. *Emerg. Infect. Dis.* 28, 2575–2577. <https://doi.org/10.3201/eid2812.221304>.
20. Muik, A., Lui, B.G., Quandt, J., Diao, H., Fu, Y., Bacher, M., Gordon, J., Toker, A., Grosser, J., Ozhelvaci, O., et al. (2023). Progressive loss of conserved spike protein neutralizing antibody sites in Omicron sublineages is balanced by preserved T cell immunity. *Cell Rep.* 42, 112888. <https://doi.org/10.1016/j.celrep.2023.112888>.
21. Lassauniere, R., Polacek, C., Utiko, M., Sorensen, K.M., Baig, S., Ellegaard, K., Escobar-Herrera, L.A., Fomsgaard, A., Spiess, K., Gunalan, V., et al. (2023). Virus isolation and neutralisation of SARS-CoV-2 variants BA.2.86 and EG.5.1. *Lancet Infect. Dis.* 23, e509–e510. [https://doi.org/10.1016/S1473-3099\(23\)00682-5](https://doi.org/10.1016/S1473-3099(23)00682-5).
22. Planas, D., Bruel, T., Staropoli, I., Guivel-Benhassine, F., Porrot, F., Maes, P., Grzelak, L., Prot, M., Mougari, S., Planchais, C., et al. (2022). Resistance of Omicron Subvariants BA.2.75.2, BA.4.6 and BQ.1.1 to Neutralizing Antibodies. Preprint at bioRxiv. <https://doi.org/10.1101/2022.11.17.516888>.
23. Park, Y.J., Pinto, D., Walls, A.C., Liu, Z., De Marco, A., Benigni, F., Zatta, F., Silacci-Fregni, C., Bassi, J., Sprouse, K.R., et al. (2022). Imprinted antibody responses against SARS-CoV-2 Omicron sublineages. *Science* 378, 619–627. <https://doi.org/10.1126/science.adc9127>.
24. Marking, U., Havervall, S., Norin, N.G., Bladh, O., Christ, W., Gordon, M., Ng, H., Blom, K., Phillipson, M., Mangsbo, S., et al. (2023). Correlates of protection and viral load trajectories in omicron breakthrough infections in triple vaccinated healthcare workers. *Nat. Commun.* 14, 1577. <https://doi.org/10.1038/s41467-023-36984-1>.
25. Seaman, M.S., Siedner, M.J., Boucau, J., Lavine, C.L., Ghantous, F., Liew, M.Y., Mathews, J.I., Singh, A., Marino, C., Regan, J., et al. (2022). Vaccine breakthrough infection leads to distinct profiles of neutralizing antibody responses by SARS-CoV-2 variant. *JCI Insight* 7, e159944. <https://doi.org/10.1172/jci.insight.159944>.
26. Lin, Y., Wu, P., Tsang, T.K., Wong, J.Y., Lau, E.H.Y., Yang, B., Leung, G.M., and Cowling, B.J. (2023). Viral kinetics of SARS-CoV-2 following onset of COVID-19 in symptomatic patients infected with the ancestral strain and omicron BA.2 in Hong Kong: a retrospective observational study. *Lancet Microbe* 4, e722–e731. [https://doi.org/10.1016/S2666-5247\(23\)00146-5](https://doi.org/10.1016/S2666-5247(23)00146-5).
27. Swadling, L., Diniz, M.O., Schmidt, N.M., Amin, O.E., Chandran, A., Shaw, E., Pade, C., Gibbons, J.M., Le Bert, N., Tan, A.T., et al. (2022). Pre-existing polymerase-specific T cells expand in abortive seronegative SARS-CoV-2. *Nature* 601, 110–117. <https://doi.org/10.1038/s41586-021-04186-8>.
28. Kundu, R., Narean, J.S., Wang, L., Fenn, J., Pillay, T., Fernandez, N.D., Conibear, E., Koycheva, A., Davies, M., Tolosa-Wright, M., et al. (2022). Cross-reactive memory T cells associate with protection against SARS-CoV-2 infection in COVID-19 contacts. *Nat. Commun.* 13, 80. <https://doi.org/10.1038/s41467-021-27674-x>.
29. Eser, T.M., Baranov, O., Huth, M., Ahmed, M.I.M., Deák, F., Held, K., Lin, L., Pekayvaz, K., Leunig, A., Nicolai, L., et al. (2023). Nucleocapsid-specific T cell responses associate with control of SARS-CoV-2 in the upper airways before seroconversion. *Nat. Commun.* 14, 2952. <https://doi.org/10.1038/s41467-023-38020-8>.
30. Tarke, A., Coelho, C.H., Zhang, Z., Dan, J.M., Yu, E.D., Methot, N., Bloom, N.I., Goodwin, B., Phillips, E., Mallal, S., et al. (2022). SARS-CoV-2 vaccination induces immunological T cell memory able to cross-recognize variants from Alpha to Omicron. *Cell* 185,

- 847–859.e11. <https://doi.org/10.1016/j.cell.2022.01.015>.
31. Keeton, R., Tincho, M.B., Ngomti, A., Baguma, R., Benede, N., Suzuki, A., Khan, K., Cele, S., Bernstein, M., Karim, F., et al. (2022). T cell responses to SARS-CoV-2 spike cross-recognize Omicron. *Nature* 603, 488–492. <https://doi.org/10.1038/s41586-022-04460-3>.
  32. Chen, X., Xu, Y., Xie, Y., Song, W., Hu, Y., Yisimayi, A., Yang, S., Shao, F., Geng, L., Wang, Y., et al. (2023). Protective effect of plasma neutralization from prior SARS-CoV-2 Omicron infection against BA.5 subvariant symptomatic reinfection. *Lancet Reg. Health West. Pac.* 33, 100758. <https://doi.org/10.1016/j.lanwpc.2023.100758>.
  33. Lin, M., Cao, K., Xu, F., Wu, X., Shen, Y., Lu, S., Kuang, Z., Ding, H., Yuan, S., Shao, M., et al. (2023). A follow-up study on the recovery and reinfection of Omicron COVID-19 patients in Shanghai, China. *Emerg. Microbes Infect.* 12, 2261559. <https://doi.org/10.1080/22221751.2023.2261559>.
  34. Chen, J.J., Li, L.B., Peng, H.H., Tian, S., Ji, B., Shi, C., Qian, C., Jiang, W.G., Liu, M.C., Li, T.T., et al. (2023). Neutralization against XBB.1 and XBB.1.5 after omicron subvariants breakthrough infection or reinfection. *Lancet Reg. Health West. Pac.* 33, 100759. <https://doi.org/10.1016/j.lanwpc.2023.100759>.
  35. Planas, D., Staropoli, I., Porot, F., Guivel-Benhassine, F., Handala, L., Prot, M., Bolland, W.H., Puech, J., Péré, H., Veyer, D., et al. (2022). Duration of BA.5 neutralization in sera and nasal swabs from SARS-CoV-2 vaccinated individuals, with or without omicron breakthrough infection. *Med (N Y)* 3, 838–847.e3. <https://doi.org/10.1016/j.medj.2022.09.010>.
  36. Yisimayi, A., Song, W., Wang, J., Jian, F., Yu, Y., Chen, X., Xu, Y., Yang, S., Niu, X., Xiao, T., et al. (2023). Repeated Omicron Exposures Override Ancestral SARS-CoV-2 Immune Imprinting. Preprint at bioRxiv. <https://doi.org/10.1101/2023.05.01.538516>.
  37. Baerends, E.A.M., Hvidt, A.K., Reekie, J., Søgaard, O.S., Stærke, N.B., Raben, D., Nielsen, H., Petersen, K.T., Juhl, M.R., Johansen, I.S., et al. (2023). SARS-CoV-2 vaccine-induced antibodies protect against Omicron breakthrough infection. *iScience* 26, 107621. <https://doi.org/10.1016/j.isci.2023.107621>.
  38. Perez-Alos, L., Hansen, C.B., Almagro Armenteros, J.J., Madsen, J.R., Heftdal, L.D., Hasselbalch, R.B., Pries-Heje, M.M., Bayarri-Olmos, R., Jarlhelt, I., Hamm, S.R., et al. (2023). Previous immunity shapes immune responses to SARS-CoV-2 booster vaccination and Omicron breakthrough infection risk. *Nat. Commun.* 14, 5624. <https://doi.org/10.1038/s41467-023-41342-2>.
  39. Zeng, C., Evans, J.P., King, T., Zheng, Y.M., Oltz, E.M., Whelan, S.P.J., Saif, L.J., Peeples, M.E., and Liu, S.L. (2022). SARS-CoV-2 spreads through cell-to-cell transmission. *Proc. Natl. Acad. Sci. USA* 119, e2111400119. <https://doi.org/10.1073/pnas.2111400119>.
  40. McMahan, K., Yu, J., Mercado, N.B., Loos, C., Tostanoski, L.H., Chandrashekar, A., Liu, J., Peter, L., Atyeo, C., Zhu, A., et al. (2021). Correlates of protection against SARS-CoV-2 in rhesus macaques. *Nature* 590, 630–634. <https://doi.org/10.1038/s41586-020-03041-6>.
  41. Gao, Y., Cai, C., Grifoni, A., Müller, T.R., Niessl, J., Olofsson, A., Humbert, M., Hansson, L., Österborg, A., Bergman, P., et al. (2022). Ancestral SARS-CoV-2-specific T cells cross-recognize the Omicron variant. *Nat. Med.* 28, 472–476. <https://doi.org/10.1038/s41591-022-01700-x>.
  42. Toda, M., Yoshifuji, A., Nakayama, T., Mise-Omata, S., Oyama, E., Uwamino, Y., Namkoong, H., Komatsu, M., Yoshimura, A., Hasegawa, N., et al. (2023). Cellular and Humoral Immune Responses after Breakthrough Infection in Patients Undergoing Hemodialysis. *Vaccines (Basel)* 11, 1214. <https://doi.org/10.3390/vaccines11071214>.
  43. Ozbay Kurt, F.G., Lepper, A., Gerhards, C., Roemer, M., Lasser, S., Arkhypov, I., Bitsch, R., Bugert, P., Altevogt, P., Gouttefangeas, C., et al. (2022). Booster dose of mRNA vaccine augments waning T cell and antibody responses against SARS-CoV-2. *Front. Immunol.* 13, 1012526. <https://doi.org/10.3389/fimmu.2022.1012526>.
  44. Painter, M.M., Johnston, T.S., Lundgreen, K.A., Santos, J.J.S., Qin, J.S., Goel, R.R., Apostolidis, S.A., Mathew, D., Fulmer, B., Williams, J.C., et al. (2023). Prior vaccination promotes early activation of memory T cells and enhances immune responses during SARS-CoV-2 breakthrough infection. *Nat. Immunol.* 24, 1711–1724. <https://doi.org/10.1038/s41590-023-01613-y>.
  45. Koutsakos, M., Reynaldi, A., Lee, W.S., Nguyen, J., Amaraseena, T., Tairaroa, G., Kinsella, P., Liew, K.C., Tran, T., Kent, H.E., et al. (2023). SARS-CoV-2 breakthrough infection induces rapid memory and *de novo* T cell responses. *Immunity* 56, 879–892.e4. <https://doi.org/10.1016/j.immuni.2023.02.017>.
  46. Wang, J., Li, K., Mei, X., Cao, J., Zhong, J., Huang, P., Luo, Q., Li, G., Wei, R., Zhong, N., et al. (2022). SARS-CoV-2 vaccination-infection pattern imprints and diversifies T cell differentiation and neutralizing response against Omicron subvariants. *Cell Discov.* 8, 136. <https://doi.org/10.1038/s41421-022-00501-3>.
  47. Li, Y., Wang, X., Shen, X.R., Geng, R., Xie, N., Han, J.F., Zhang, Q.M., Shi, Z.L., and Zhou, P. (2022). A 1-year longitudinal study on COVID-19 convalescents reveals persistence of anti-SARS-CoV-2 humoral and cellular immunity. *Emerg. Microbes Infect.* 11, 902–913. <https://doi.org/10.1080/22221751.2022.2049984>.
  48. Pusnik, J., Monzon-Posadas, W.O., Zorn, J., Peters, K., Baum, M., Proksch, H., Schluter, C.B., Alter, G., Menting, T., and Streeck, H. (2023). SARS-CoV-2 humoral and cellular immunity following different combinations of vaccination and breakthrough infection. *Nat. Commun.* 14, 572. <https://doi.org/10.1038/s41467-023-36250-4>.
  49. Grifoni, A., Sidney, J., Vita, R., Peters, B., Crotty, S., Weiskopf, D., and Sette, A. (2021). SARS-CoV-2 human T cell epitopes: Adaptive immune response against COVID-19. *Cell Host Microbe* 29, 1076–1092. <https://doi.org/10.1016/j.chom.2021.05.010>.
  50. Mateus, J., Dan, J.M., Zhang, Z., Rydzynski Moderbacher, C., Lammers, M., Goodwin, B., Sette, A., Crotty, S., and Weiskopf, D. (2021). Low-dose mRNA-1273 COVID-19 vaccine generates durable memory enhanced by cross-reactive T cells. *Science* 374, eabj9853. <https://doi.org/10.1126/science.abj9853>.

STAR★METHODS

KEY RESOURCES TABLE

REAGENT or RESOURCE	SOURCE	IDENTIFIER
<b>Antibodies</b>		
anti-human CD3 BUV661 (UCHT1)	BD Biosciences	Cat# 612965; RRID: AB_2916886
anti-human CD4 BV510 (RPA-T4)	BioLegend	Cat# 300546; RRID: AB_2563314
anti-human CD8a BV785 (RPA-T8)	BioLegend	Cat# 301046; RRID: AB_2563264
anti-human CD14 R718 (M5E2)	BD Biosciences	Cat# 567069; RRID: AB_2916417
anti-human CD19 FITC (4G7)	BioLegend	Cat# 392508; RRID: AB_2750099
anti-human CD69 allophycocyanin (APC) (FN50)	BioLegend	Cat# 310910; RRID: AB_314845
anti-human OX40 phycoerythrin (PE)/Dazzle 594 (ACT35)	BioLegend	Cat# 350020; RRID: AB_2571940
anti-human CD137 BV421 (4B4-1)	BioLegend	Cat# 309820; RRID: AB_2563830
anti-human CD45RA PE/Cy7 (HI100)	BioLegend	Cat# 304126; RRID: AB_10708879
anti-human CCR7 BV605 (3D12)	BD Biosciences	Cat# 353224; RRID: AB_2561753
anti-human IL-2 BV711 (MQ1-17H12)	BioLegend	Cat# 500346; RRID: AB_2616639
anti-human IFN- $\gamma$ PE (B27)	BioLegend	Cat# 506507; RRID: AB_315440
anti-human TNF- $\alpha$ BV650 (MAb11)	BioLegend	Cat# 502938; RRID: AB_2562741
anti-human CD28 (CD28.2)	BioLegend	Cat# 302902; RRID: AB_314304
anti-human CD49d (9F10)	BioLegend	Cat# 304334; RRID: AB_2749896
Live/Dead Viability FVS780	BD Biosciences	Cat# 565388; RRID: AB_2869673
<b>Bacterial and virus strains</b>		
SARS-CoV-2 pseudovirus for D614G	This study	N/A
SARS-CoV-2 pseudovirus for BA.2	This study	N/A
SARS-CoV-2 pseudovirus for BA.4/5	This study	N/A
SARS-CoV-2 pseudovirus for BF.7	This study	N/A
SARS-CoV-2 pseudovirus for BQ.1.1	This study	N/A
SARS-CoV-2 pseudovirus for BA.2.75.2	This study	N/A
SARS-CoV-2 pseudovirus for CH.1.1	This study	N/A
SARS-CoV-2 pseudovirus for XBB.1.5	This study	N/A
SARS-CoV-2 pseudovirus for XBB.1.16	This study	N/A
SARS-CoV-2 pseudovirus for EG.5.1	This study	N/A
SARS-CoV-2 pseudovirus for JN.1	This study	N/A
SARS-CoV-2 WT/human/CHN/Beijing_IME-BJ01/2020	This study	Genbank No. MT291831
SARS-CoV-2 Omicron BA.2 CoV/human/CHN_CVRI-04/2022	This study	N/A
SARS-CoV-2 Omicron BA.5 CoV/human/CHN_CVRI-12/2022	This study	N/A
SARS-CoV-2 XBB.1.16 CoV/human/CHN_CVRI-06/2023	This study	N/A
<i>E. coli</i> DH5 $\alpha$ Competent Cells	TaKaRa	Cat# 9057
<b>Biological samples</b>		
Human blood samples	This study	N/A
<b>Chemicals, peptides, and recombinant proteins</b>		
Omicron BA.2 spike mega peptide pool	GLBiochem	N/A
Omicron CH.1.1 spike mega peptide pool	GLBiochem	N/A
SARS-CoV-2 Omicron BA.2 Spike Trimer Protein	ACROBiosystems	Cat# SPN-C522b
SARS-CoV-2 Omicron CH.1.1 Spike Trimer Protein	ACROBiosystems	Cat# SPN-C522j
Luciferase Assay System	Vazyme	Cat# DD1204-02

(Continued on next page)



**Continued**

REAGENT or RESOURCE	SOURCE	IDENTIFIER
Cell Activation Cocktail	BioLegend	Cat# 423301
Brefeldin A	BioLegend	Cat# 420601
Monensin	BioLegend	Cat# 420701
Cyto-Fast™ Fix/Perm Buffer	BioLegend	Cat# 426803
Cell Staining Buffer	BioLegend	Cat# 420201

**Experimental models: Cell lines**

293T-ACE2 cells	Vazyme	Cat# DD1701-01
HEK-293T cells	ATCC	Cat# CRL-3216
Vero E6	ATCC	Cat# CRL-1586

**Software and algorithms**

GraphPad Prism Version 8.0.2	GraphPad Software	<a href="https://www.graphpad.com">https://www.graphpad.com</a>
ID7000 Software	TreeStar	<a href="https://www.sonybiotechnology.com/us/instruments/id7000-spectral-cell-analyzer/software/">https://www.sonybiotechnology.com/us/instruments/id7000-spectral-cell-analyzer/software/</a>
Rstudio	Posit	<a href="https://www.rstudio.com/categories/rstudio-ide/">https://www.rstudio.com/categories/rstudio-ide/</a>

**RESOURCE AVAILABILITY**

**Lead contact**

Further information and requests for resources and reagents should be directed to and will be fulfilled by the lead contact, Dr. Guo-Lin Wang ([guolin\\_wang2019@163.com](mailto:guolin_wang2019@163.com)).

**Materials availability**

Aliquots of synthesized sets of peptides utilized in this study will be made available upon request. There are restrictions to the availability of the peptide reagents due to cost and limited quantity.

**Data and code availability**

The published article includes all data generated or analyzed during this study, and summarized in the accompanying tables, figures and [supplemental information](#). This paper does not report original code. Any additional information required to reanalyze the data reported in this paper is available from the [lead contact](#) upon request.

**EXPERIMENTAL MODEL AND STUDY PARTICIPANT DETAILS**

**Study participants**

A cohort of 42 participants with confirmed Omicron BA.2.2 infections was enrolled in Jiangyin city, Jiangsu Province of China between September 19 and November 08, 2022 in this study. The median age of the participants was 49.0. 23 (54.8%) subjects were male and 19 (45.2%) subjects were female. In addition, ten vaccinated subjects (five males and five females, with a median age of 40.5) without infection were enrolled as healthy controls. The race of all enrolled participants was the Asian. Information on age, sex and vaccination background of these participants were listed in [Tables 1](#) and [S1](#).

**Ethics statement**

The study was approved by the Institutional Review Board of the Beijing Institute of Microbiology and Epidemiology (IRB number: AF/SC-08/02.245). Written informed consent was obtained from all participants.

**METHOD DETAILS**

**Peripheral blood mononuclear cells (PBMCs) isolation**

The PBMCs were isolated using SepMate™-15 (STEMCELL Technologies Inc., Vancouver, Canada) density gradient centrifugation according to the manufacturer's instructions. Blood samples, PBS+2% FBS, and density gradient medium were firstly mixed with equal volume. Then the diluted samples were centrifuged at 1200×g for 10 min at room temperature. PBMCs were poured into a separate 15 ml tube and washed twice with PBS+2% FBS. Finally, the PBMCs were resuspended with serum-free cell cryopreservation solution (New Cell & Molecular Biotech Co., Ltd, Cat# C40100) and stored at -80°C until use.

### Enzyme-linked immunosorbent assay analysis of IgG antibody to spike trimer of Omicron BA.2 and BA.5

The recombinant spike trimer of Omicron BA.2 (ACROBiosystems, Cat# SPN-C522b) and BA.5 (ACROBiosystems, Cat# SPN-C522j) was coated onto flat-bottom, 96-well, enzyme-linked immunosorbent assay (ELISA) plates overnight at 4°C with 0.1 µg/well. The plates were then washed with PBS with 0.05% Tween 20 (PBS-T) and blocked with blocking buffer (2% bovine serum albumin in PBS) for one hour at room temperature. Duplicate 3-fold 8-point serial dilutions (starting at 1:200) of heat-inactivated serum samples diluted in blocking buffer were added to the wells and incubated at 37°C for 1 hour. Following that, the wells were incubated with the 1:5000 horseradish peroxidase (HRP)-labeled anti-human IgG antibody (Promega, Cat# W4031) and TMB substrate (Mei5bio, Cat# MF142-01). The optical density (OD) was measured by a spectrophotometer at wavelengths of both 450 nm and 630 nm. Endpoint antibody titers were calculated by fitting a curve using 4 parameter log regression analysis, and the initial dilution of 200 was considered as the detection threshold.

### Production of variant SARS-CoV-2 spike plasmid pseudovirus

SARS-CoV-2 pseudoviruses were generated by co-transfecting HEK-293T cells (ATCC, Cat# CRL-3216) with human immunodeficiency virus backbones expressing firefly luciferase (pNL4-3-R-E-luciferase) and pcDNA3.1 vector encoding either D614G, BA.2, BA.5, BF.7, BQ.1.1, BA.2.75.2, CH.1.1, XBB.1.5, XBB.1.16, EG.5.1, or JN.1 S proteins plasmid.<sup>34</sup> The medium was replaced with fresh medium at 24 hours, and the supernatants were harvested at 48 hours post-transfection and clarified by centrifugation at 400 g for 10 minutes before aliquoting and storing at -80°C until use.

### Pseudovirus neutralization test

Pseudoviruses were titrated on 293T-ACE2 cells (Vazyme, Cat# DD1701-01) prior to conducting the neutralization assays to normalize the viral input between assays. Heat-inactivated sera were serially diluted starting from 1:30 with a dilution factor of three. Then, 50 µL of diluted pseudovirus was added and incubated with diluted serum for 1 hour at 37°C. After that,  $2 \times 10^4$  293T-ACE2 cells per well were added and incubated at 37°C, 5% CO<sub>2</sub> for 48 hours. Subsequently, luciferase activity was quantified using the Luciferase Assay System (Vazyme, Cat# DD1204-02) using GloMax 96 Microplate Luminometer (Promega, E6521). Neutralization ID<sub>50</sub> values for serum were calculated by a four-parameter nonlinear regression inhibitor curve in GraphPad Prism 8.0.2 (version 8.0.2, La Jolla, California, USA). A sample with ID<sub>50</sub> values no more than 30 (the detectable limit) was considered negative for neutralizing antibodies and was assigned a value of 10 in geometric mean titer (GMT) calculations.

### Live-virus neutralization test

To further confirm the results by pVNT, we measured the serum neutralizing antibody by a live-virus neutralizing assay (LVNT). Briefly, the serum was heat-inactivated at 56°C for 30 min. Serum were then serially diluted starting from 1:10 with a dilution factor of two, and an equal volume of challenge virus solution containing 100 TCID<sub>50</sub> of virus (SARS-CoV-2 WT/human/CHN/Beijing\_IME-BJ01/2020, SARS-CoV-2 Omicron BA.2 CoV/human/CHN\_CVRI-04/2022, SARS-CoV-2 Omicron BA.5 CoV/human/CHN\_CVRI-12/2022, or SARS-CoV-2 XBB.1.16 CoV/human/CHN\_CVRI-06/2023) was added. After 1 hour incubation at 37°C, 5% CO<sub>2</sub>, 100 µL of  $1 \times 10^5$  cells/mL Vero E6 cells were added to the wells of the virus-serum mixture and then cultured in a CO<sub>2</sub> incubator at 37°C for 4 days. After that, the cytopathic effect (CPE) was read. The Reed-Muench method was used to calculate the neutralization endpoint (convert the serum dilution to logarithm), which means that the highest dilution of serum that can protect 50% of cells from infection by challenge with 100 TCID<sub>50</sub> virus is the antibody potency of the serum. For final titer lower than 10, a value of 5 was assigned for geometric mean calculations and was considered seronegative.

### Antigenic Cartography

The neutralizing data of participants in BTI T1 group and BTI plus RI T2 group was used to generate the antigenic map with R package Rac-macs (version 1.1.9) and ggplot2 (version 3.4.2). The spacing of the grid lines corresponds to the neutralizing antibody titers unit, which was equivalent to the 2-fold change in the neutralizing ID<sub>50</sub> titer.

### SARS-CoV-2 BA.2 and CH.1.1 spike peptide synthesis and pooling

Peptides were synthesized against whole spike protein of SARS-CoV-2 BA.2.2 and CH.1.1 omicron subvariants. Peptides were 15-mers overlapping by 10 amino acids and were synthesized in GL Biochem Ltd. (Shanghai, China). All peptides were individually responded in dimethyl sulfoxide (DMSO) at a concentration of 10 mg/ml. Megapools (MP) for each variants spike were created by pooling aliquots of these individual peptides, and resuspending in DMSO at a concentration of 1 mg/ml. The detailed information of the peptides was available in [Table S3](#).

### Flow cytometry-based T cell assays

The activation induced cell marker (AIM) and Intra Cellular Staining (IC) assay was conducted as previous described.<sup>49,50</sup> In summary, PBMCs were cultured in the presence of 1 µg/ml SARS-CoV-2 spike MPs, 0.5 µg/ml CD28 (BioLegend, Cat# 302902), and 0.5 µg/ml CD49d (BioLegend, Cat# 304334) in 96-well U-bottom plates at a concentration of  $1 \times 10^6$  PBMC per well. As negative and positive controls, DMSO and Cell Activation Cocktail (BioLegend, Cat# 423301) was used to stimulate the cells, respectively. After incubation for 19 hours at 37°C, 5% CO<sub>2</sub>, Brefeldin A (BFA, BioLegend, Cat# 420601) and Monensin (BioLegend, Cat# 420701) were added to cells for blocking cytokine transport. After five hours, the cells were stained with CD3 BUV661 (BD, Cat# 612965), CD4 BV510 (BioLegend, Cat# 300546), CD8a

(BioLegend, Cat# 301046), CD19 (BioLegend, Cat# 392508), CD14 (BD, Cat# 567069), CD69 (BioLegend, Cat# 310910), OX40 (BioLegend, Cat# 350020), CD137 (BioLegend, Cat# 309820), CCR7 (BD, Cat# 568681), CD45RA (BioLegend, Cat# 304126), and Live/Dead FSV780 (BD, Cat# 565388). Cells were then fixed using Cyto-Fast™ Fix/Perm Buffer (BioLegend, Cat# 426803) and stained with IL-2 (BioLegend, Cat# 500346), IFN- $\gamma$  (BioLegend, Cat# 506507), and TNF- $\alpha$  (BioLegend, Cat# 502938). Finally, cells were fixed in Cell Staining Buffer (BioLegend, Cat# 420201).

All samples were acquired on a ID7000TM Cell Analyzer (Sony Biotechnology) and analyzed with ID7000 Software (<https://www.sonybiotechnology.com/us/instruments/id7000-spectral-cell-analyzer/software/>). A representative example of the gating strategy for AIM and ICS assays is showed in Figure S5. Virus-specific AIM CD4<sup>+</sup> and CD8<sup>+</sup> T cells responses were calculated as percent of total CD4<sup>+</sup> (OX40<sup>+</sup>CD137<sup>+</sup>) or CD8<sup>+</sup> (CD69<sup>+</sup>CD137<sup>+</sup>) T cells. For ICS, CD3<sup>+</sup>CD4<sup>+</sup> and CD3<sup>+</sup>CD8<sup>+</sup> cells were further gated based on a combination of each cytokine (IFN- $\gamma$ , TNF- $\alpha$ , IL-2) with FSC-A, respectively. The background was removed from the data by subtracting the wells stimulated with DMSO. The values above zero are considered as positive.

### QUANTIFICATION AND STATISTICAL ANALYSIS

The data was described using descriptive statistics, which display continuous variables as Geometric mean or medians, categorical variables as percentages or proportions. The "n" in the figure or figure legends represents the number of enrolled participants. The statistical analyses were performed using GraphPad Prism (version 8.0.2) and RStudio (version 4.2.3) software. Differences between the groups were assessed by either the Mann-Whitney test or the Wilcoxon matched-pairs signed rank test. The strength of correlations was evaluated by Spearman's test. All statistical tests were 2-sided with a significance level of 0.05. Significance value is denoted as "\*" in Figures 3 and 7, where \* indicates  $p \leq 0.05$ , \*\* indicates  $p < 0.01$ , \*\*\* indicates  $p < 0.001$ , \*\*\*\* indicates  $p < 0.0001$ .